Corrosion Science 77 (2013) 342–349

Contents lists available at ScienceDirect

Corrosion Science

journal homepage: www.elsevier.com/locate/corsci

New zinc–rare earth alloys: Influence of intermetallic compounds on the corrosion resistance

Delphine Veys-Renaux [a,*], Khadoudj Guessoum [a,b], Emmanuel Rocca [a], Nicolas David [a], Kamel Belhamel [b]

[a] *Institut Jean Lamour-UMR CNRS 7198, Université de Lorraine-CNRS, BP 70239, Vandoeuvre-lès-Nancy 54506, France*
[b] *Laboratoire des Matériaux Organiques, Département de Génie des Procédés, Faculté de Technologie, Université de Béjaia, Béjaia 06000, Algeria*

ARTICLE INFO

Article history:
Received 7 March 2013
Accepted 29 August 2013
Available online 6 September 2013

Keywords:
A. Zinc
A. Rare earth elements
A. Intermetallics
C. Thermodynamic diagrams
B. SEM
B. Polarization

ABSTRACT

New ZnRE 1–2 wt.% alloys (RE = Ce, La and Mischmetal) were synthesized. Microstructural analyses reveal that rare-earth metals are exclusively present in intermetallic phases contained within the zinc matrix: $CeZn_{11}$ or $LaZn_{13}$ in binary alloys; $Ce_{1-x}La_xZn_{11}$ and $Ce_yLa_{1-y}Zn_{13}$ in Zn–Mischmetal alloys. This phase equilibrium is confirmed by a thermodynamic description of the Zn-rich corner of Zn–Ce–La system. Both intermetallic phases $CeZn_{11}$ and $LaZn_{13}$ induce a cathodic inhibition of the corrosion of the Zn–RE alloys in comparison with pure zinc. In the specific case of cerium addition, a significant anodic inhibition is also observed.

1. Introduction

In the field of cathodic protection of steel structures exposed to atmospheric and marine media, zinc is extensively used. Actually, compared to other metals with low redox potentials (like aluminum and magnesium), zinc is electrochemically active in a wide range of media but keep a relatively low dissolution rate, so that the life-time of the sacrificial anode in zinc or coating is satisfactory in many environments [1]. Nevertheless, the addition of alloying elements, besides the improvement of workability, is necessary to enhance the mechanical properties and the corrosion resistance of zinc in practice [2]. Indeed, the natural corrosion layer on zinc, named "white rust", is generally composed of voluminous, lamellar and not well adherent products as hydrozincite $Zn_5(CO_3)_2(OH)_6$, zinc hydroxysulfate $Zn_4SO_4(OH)_6{\cdot}4H_2O$, zinc hydroxychloride $Zn_5(OH)_8Cl_2{\cdot}H_2O$ [3,4], that are poorly protective.

In the case of nickel, cobalt or manganese addition to zinc, the improvement of corrosion protection is generally attributed to a selective dissolution leading to a surface enrichment in alloying element, which reduces the rate of white rust formation [5,6]. In case of aluminum addition, the corrosion of alloys induces the formation of a double lamellar hydroxide, namely $Zn_6Al_2CO_3(OH)_{16}{\cdot}4H_2O$, that inhibits the growth of crumbly white rust [7] .

Further addition of small amounts of rare-earth elements to ZnAl 5 wt.% alloy improves its corrosion resistance through the formation of a "lanthanide-doped" corrosion products layer according to Rosalbino's studies [8,9]. In these alloys the rare earth seems to be present in ternary intermetallic phases according to their analysis. Recently, an electrochemical study of Zn–Ce alloys in corrosive medium has shown that an optimum concentration of cerium, around 2 wt.%, is necessary to reach a optimum in corrosion resistance [10].

In all cases, the change in the chemical composition or in the growth rate of the corrosion products induce a modification of the morphology of the corrosion layer and an improvement of its adhesion, which lead to a decrease of the corrosion rate compared to the pure zinc.

On the other hand, many studies point out that the effect of alloying elements is also very dependent on their distribution in the alloy, and especially the distribution of the different intermetallic phases containing the alloying element [11–13].

The purpose of this work is thus to study the possibility to reinforce the natural corrosion products of zinc by alloying zinc with cerium, lanthanum and mischmetal (Ce/La: 75/25 wt.%). New zinc–cerium, zinc–lanthanum and zinc–lanthanum–cerium alloys were synthesized until 2 wt.% in rare-earth elements. The microstructure of the alloys, analyzed by scanning electron microscopy (SEM), electron micro-probe analysis (EPMA) and X-ray diffraction (XRD), is compared to the thermodynamic data of the phase diagrams. In the case of Zn-La-Ce system, a modeling of the Zn-rich corner is proposed in this paper.

Then, the effect of rare earth elements on the corrosion behavior of the alloys was investigated in aerated corrosive reference water

---

* Corresponding author. Tel.: +33 3 83 68 46 30.
E-mail address: delphine.veys-renaux@univ-lorraine.fr (D. Veys-Renaux).

0010-938X/$ - see front matter © 2013 Elsevier Ltd. All rights reserved.
http://dx.doi.org/10.1016/j.corsci.2013.08.024

(simulating wet/dry cycles under environmental exposure) by using different stationary electrochemical methods. In order to understand the electrochemical relation between the intermetallic phases and the zinc matrix and to highlight the specificities of these new alloys, pure intermetallic phases synthesized as bulk material were also studied.

2. Experimental details

2.1. Synthesis and characterization of alloys and pure intermetallic phases

ZnRE 1–2 wt.% alloys (RE = Ce, La and Mischmetal: Ce 75 wt.%/La 25 wt.%) as well as RE-enriched pure intermetallic phases ($CeZn_{11}$ and $LaZn_{13}$) investigated in this work were synthesised from cerium pieces (99.999 wt.% nominal purity), lanthanum pieces (99.9999 wt.% nominal purity), mischmetal pieces (Ce 75 wt.%–La 25 wt.%) and pure zinc (99.9999 wt.% nominal purity), supplied by Alfa Aesar. Rare earth metals were cut and abraded under oil and washed with n-hexane. The alloys and pure intermetallic phases were prepared into closed alumina crucibles (Al_2O_3), using a vertical Pyrox furnace maintained at 600 °C during 24 h under pure argon flux, to prevent oxidation of metals and volatilization of zinc. Then, the ingots of alloys were re-melted in a muffle furnace at 550 °C for 20 min under a nitrogen atmosphere, to be rapidly cast in plates in an aluminum mold (60 × 60 × 3 mm) under atmospheric conditions. After synthesis, the samples were analyzed by X-ray diffraction with a classical diffractometer (X'Pert Pro/Philips), using Cu $K\alpha_1$ wavelength ($\lambda_1 = 1.54051$ nm) in Bragg–Brentano geometry. Microstructures of zinc alloys were investigated by backscattered scanning electron microscopy (SEM: Philips XL30) and analyzed by electron probe micro-analysis (micro-probe: CAMECA SX100). Each elemental analysis by EPMA is the average of ten different analysis points.

2.2. Thermodynamic calculations

The zinc corner of Ce–La–Zn diagram was modeled from the thermodynamic data of binary diagrams of literature. The Ce–Zn and La–Zn systems were respectively optimized by Wang et al. [14] and Qi et al. [15] according to the CALPHAD method [16]. According to several previous works [17,18], an optimized phase diagram for Ce–La system was calculated in this work and is presented in Fig 1a. The optimized coefficients obtained for Ce–La system are reported in Table 1.

In the Ce–La–Zn system, liquid, body-centered cubic (BCC A2), face-centered cubic (FCC A1), hexagonal close-packed (HCP A3) and double hexagonal close-packed (DHCP) are described with the substitutional solution model with excess terms described by the Redlich–Kister polynomials. Disordered substitutional solutions are represented by only one sublattice where all the atoms mix together. Concerning $CeZn_2$, $CeZn_5$, $CeZn_{11}$, Ce_2Zn_{17} and Ce_3Zn_{22} stoichiometric compounds and regarding the similarities of their respective crystallographic data with their respective opposite in the La–Zn border ($LaZn_2$, $LaZn_5$, $LaZn_{11}$, La_2Zn_{17} and La_3Zn_{22}), they are described as ternary solution phases with substitution of Ce by La at Zn ratio constant and treated as the formula $(Ce,La)_aZn_b$. All other intermediate compounds are modeled as stoichiometric compounds, namely CeZn, $CeZn_3$, Ce_3Zn_{11}, $Ce_{13}Zn_{58}$, $LaZn_4$, $LaZn_{13}$. The Gibbs energies of the pure elements, referred to the enthalpy of each element in its so-called standard element reference (SER) state (the stable state at 10^5 Pa and 298.15 K) were taken from the SGTE Pure Element (unary) Database [19].

The calculated Zn-rich corner of the Ce–La–Zn phases diagram is presented in Fig. 1b and the obtained set of parameters is summarized in Table 1.

2.3. Electrochemical characterisations

Electrochemical characterisations were carried out both on ZnRE alloys and on the pure $CeZn_{11}$ and $LaZn_{13}$ intermetallic phases after mechanical abrading on SiC paper up to grade 4000 and mirror-like polishing with 1 µm diamond paste. All the electrochemical experiments were performed in a reference corrosive solution (D 1384-87 ASTM standard water [20]: Na_2SO_4, 148 mg/l; $NaHCO_3$, 138 mg/l; NaCl, 165 mg/l (pH = 8.3; $\sigma = 650\ \mu S\ cm^{-1}$)), noted "ASTM water" in the text, whose composition simulates corrosion under environmental exposure [21,22]. The solution was

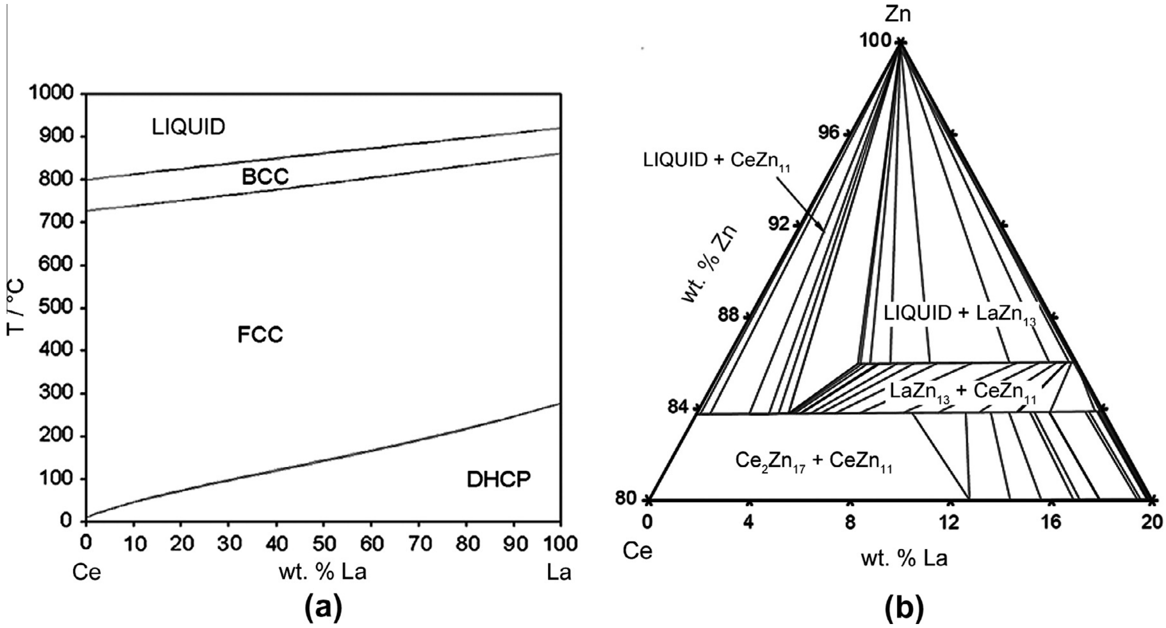

Fig. 1. Calculated phase diagram of Ce–La with optimized set of parameters based on experimental data [17,18] (a); Calculated ternary equilibria in the Zn-rich corner of the Ce–La–Zn phase diagram at 873 K based on experimental points from this work (b).